Carbohydrate Polymers 78 (2009) 794–798

Contents lists available at ScienceDirect

Carbohydrate Polymers

journal homepage: www.elsevier.com/locate/carbpol

Water soluble levan polysaccharide biopolymer electrospun fibers

Sandeep Manandhar, Shailesh Vidhate, Nandika D'Souza *

Department of Materials Science and Engineering, University of North Texas, TX, USA

ARTICLE INFO

Article history:
Received 1 June 2009
Received in revised form 16 June 2009
Accepted 22 June 2009
Available online 17 July 2009

Keywords:
Electrospinning
Levan
Biopolymer
Fibers

ABSTRACT

Electrospinning has been used to prepare nanofibers from diverse biopolymers. Here we report on preparation of fibers by electrospinning of levan (a polysaccharide) from distilled water. A high concentration of levan was required for fiber formation. This suggests that higher concentrations enable the formation of chain entanglements required to maintain the jet strength. In general, fiber diameter decreased with increased voltage, distance between collector plate and needle and decreased pump flow rate. X-ray diffraction of the fibers showed a highly amorphous character in levan formed from solution compared to the levan powder.

1. Introduction

The process of drawing polymer filaments using electrostatic force to produce textile yarns was patented in 1934 by Formhals (1934). The fibers are drawn from a solution and collected as a non-woven mat. Various biopolymers have been used to generate fibers (Du & Hsieh, 2008; Frey, 2008; Jiang, Fang, Hsiao, Chu, & Chen, 2004; Ritcharoen et al., 2008; Song, Kim, & Kim, 2008; Woerdeman et al., 2005). This trend was fueled by health and environmental concerns and the desire to replace some petrochemical feedstocks with agricultural and microbial products. However, most biopolymers have been spun from potentially harmful chemicals (due to their solubility) such as hydrochloric acid and chloroform (Desai, Kit, Li, & Zivanovic, 2008). It is important to have environmentally benign solvents concomitant with biopolymer sources to form fibers.

Levan (Fig. 1), is an exopolysaccharide with an unusually low intrinsic viscosity (0.14 dl/gm) attributed to its spherical shape (Arvidson, Rinehart, & Gadala-Maria, 2006). Spheres of the specific levan used in this study averaged 139 nm in diameter (Ploehn). The compact form is maintained in water at room temperature so solutions remain fluid while similar concentrations of other polysaccharides would form thick pastes or gels. Levan is produced by the fermentation of sucrose. The backbone is a β-2,6 polyfructan with β-2,1 bonding at branch points. Levans have a high molecular weight with this particular levan measuring 5.7×10^6 g/mol (Ploehn). The density is 1.4 g/cm^3. Levan is biodegradable and water soluble. Like many polysaccharides, levan is not soluble in most organic solvents, dimethyl sulfoxide (DMSO) being one exception. Levan decomposes prior to decomposition around 225 °C. The glass transition temperature is 141 °C.

The absence of adverse medical effects has been a noted advantage of levan. An agar diffusion test indicated that the levan used here is not cytotoxic. Both a chorioallantoic membrane vascular assay (CAMVA) and a bovine corneal opacity and permeability test (BCOP) showed that levan causes no ocular irritancy. Limited human studies revealed no dermal irritation or allergic contact sensitization resulting from exposure to levan (Combie, 2009).

The objective of this paper is to form electrospun fibers. Based on microscopic observations and viscometric behavior (Arvidson et al., 2006), it has been established that levan exists in a spherical or globular shape – not a particularly auspicious structure for electrospinning where entanglement of long chain polymers leads to fiber formation. However, the extremely low intrinsic viscosity implied minimal branching, so it was reasoned that, if properly unraveled, the backbone of fructan residues uninterrupted by other moieties might have good flexibility and the potential to be electrospun into long fibers. As reported, (Arvidson et al., 2006) for concentrations of up to 30% by mass, Levan displays Newtonian behavior. Between 30% and 55%, shear thinning behavior is observed indicating an increased role of entanglements. For greater than 55% by weight no plateau at low shear rates is obtained.

To facilitate preparation of concentrated levan solutions in water, both sonication and gentle heating were employed. The experimental parameters of electrospinning were varied to generate a series of fibers of different widths. Fibers were observed by electron microscopy. The structural differences between the powdered levan and the formed fibers were examined using X-ray diffraction (XRD).

* Corresponding author. Tel.: +1 940 565 2979.
E-mail address: ndsouza@unt.edu (N. D'Souza).

0144-8617/$ - see front matter © 2009 Elsevier Ltd. All rights reserved.
doi:10.1016/j.carbpol.2009.06.023

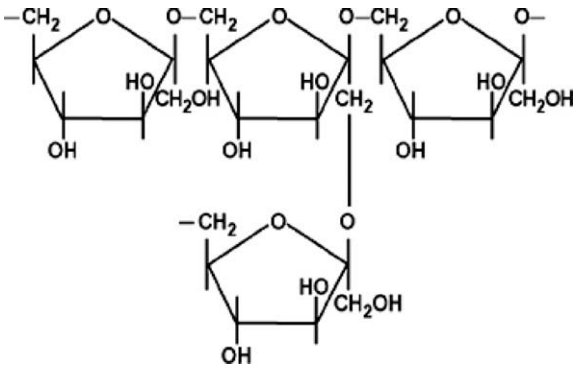

Fig. 1. Levan structure.

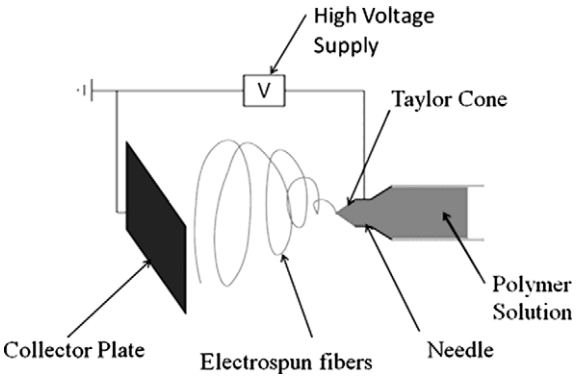

Fig. 2. Diagram of electrospinning apparatus.

2. Experimental procedure

2.1. Materials and fiber preparation

Levan was provided in powder form by Montana Polysaccharides Corp., Winnsboro, SC. Levan and deionized water were mixed by a magnetic stirrer. The levan solution was also sonicated to enhance mixing. The initial concentration was 50% levan by weight. The levan–water solution was then heated at 100 °C for about 15 min. The heat treatment helped to remove excess water and increased the concentration to 60% levan by weight. The weight percentage of the levan was determined by weighing the solution before and after heating and assuming the mass lost was water. This solution was transferred to the syringe.

Fig. 2 provides a schematic of the electrospinning setup. A 5 ml syringe made by National Scientific (Model #57510-5) was used. The needle fitted on the syringe was an 18 gauge (1.27 mm) 1" long stainless steel blunt needle with a Luer polypropylene hub. The syringe with needle was placed on a Razel syringe pump (Model #R99-FM from Razel Scientific Instruments, St. Albans, VT). Three variables were investigated, the syringe pump rate, the distance between the needle and the plate and the voltage (Table 1). The syringe pump rate of 2.29 and 3.81 cm^3/h, the distance between the needle and the plate of 10 cm, 15 cm and 20 cm and the voltage of 10, 15, 20 kV were each examined.

The solution was pumped from the syringe. The needle was then charged to the prescribed voltage using a high voltage power supply (Gamma High Voltage Research Inc., Ormond Beach, FL, Model #ES30P-5W/DAM). The collector plate was set at the prescribed distance from the needle, covered with non-stick aluminum foil and grounded.

As the syringe pump and the high voltage power supply were turned on, the polymer solution came out of the needle forming a droplet. This droplet was attracted by the electrostatic force to form a cone known as the Taylor cone (Taylor, 1969). The cone was formed due to the surface tension of the polymer solution. As the electrostatic force overcame the surface tension, the solution was ejected in the form of fibers which were dried, electrospun in the air and accumulated at the collector plate.

Various external parameters affect the electrospinning process by influencing fiber morphology. Applied voltage has a direct effect on stretching and acceleration of the polymer jet. At lower voltages reduced acceleration of the jet increases flight time and favors formation of finer fibers with better crystalline structure (Zhao, 2004). At higher voltages, there is a greater tendency for bead formation (Demir, Yilgor, & Erman, 2002). Feed rate determines the amount of solution available at the tip of needle for electrospinning. For a given voltage, there is a corresponding feedrate if a stable Taylor cone is to be maintained (Rutledge et al., 2001). The internal diameter of the needle is also an influential factor in electrospinning. A smaller internal diameter reduces clogging as well as the number of beads on the surface of the fiber (Mo, Xu, Kotaki, & Ramakrishna, 2004). Finally the distance between the collector plate and the needle affects the flight time and electrical field strength and ultimately the quality of electrospun fiber. Sufficient flight time is necessary to evaporate the solvent. Decreasing the distance has the same effect as increasing the voltage. When the distance is too large, fibers may not deposit on the collector plate. A summary of conditions under which the fiber was formed is shown in Table 1.

2.2. Scanning electron microscopy (SEM)

The fibers were removed from the collector plate for analysis. Fibers were observed using a FEI Quanta environmental scanning electron microscope. In this microscope the pressure was set to 1.17e-4 Torr. The voltage of the electron beam was 30 kV and the working distance was 8 mm. An Everhardt–Thornley Secondary Electron Detector was used. Eighty fiber dimensions were measured from micrographs collected and histograms developed and analyzed.

2.3. X-ray diffraction (XRD)

A Rigaku Ultima III refractometer system was used to perform XRD on the levan powder and levan fibers between 2 and 40 two-theta angles using a scan speed of 2 degrees per min.

Table 1
Fiber process conditions and histogram results.

Condition	1	2	3	4	5	6	7	8	9
Voltage (kV)	25	20	15	25	20	15	25	20	15
Flow rate (cc/h)	2.29 cm^3/h	2.29 cm^3/h	2.29 cm^3/h	3.81 cm^3/h	3.81 cm^3/h	3.81 cm^3/h	2.29 cm^3/h	2.29 cm^3/h	2.29 cm^3/h
Distance (cm)	15	15	15	15	15	15	10	10	10
High frequency of fibers (μm)	1–1.2	1.2–1.4	3–3.3	0.6–0.8	1.2–1.4	1.6–1.8	1.2–1.4	1.8–2	1.4–1.6
Range of fibers (μm)	0.36–3.75	0.39–4.76	1.12–7.06	0.08–1.94	0.78–4.98	0.62–7.42	0.65–2.80	0.28–4.26	0.31–3.32
Mean (μm)	1.48	1.86	3.39	1.1	2.26	2.76	1.44	1.71	1.58

3. Results and discussion

3.1. Fiber dimensional characterization

SEM images were recorded at different voltages, pump rates and distances from the plate and are shown in Fig. 3. Images were analyzed using ImageJ® Software. The diameters of fibers in the images were measured. Eighty measurements were made and the data converted into a histogram with a bin size of 0.2 μm (Fig. 4). Table 1 gives a comparison of the average fiber diameter and the breadth of the fiber dimensions, showing the effects of the change in voltage, distance and flow rate. Three parameters are tabulated – the fiber diameter range that had the highest frequency of occurrence, the breadth of the histogram and the average fiber diameter.

Some general trends are observed. Comparing conditions 1 with 7 and 2 with 8, the effect of decreasing distance between the needle and the collector plate can be determined. While the peak and mean values of the two conditions are similar, a narrowing in the breadth of the histogram with increased distance between needle and collector plate is observed. Thus at the same flow rate for 25 and 20 kV, a smaller range of fibers are obtained. When a low voltage of 15 kV is used, the same cannot be said, because the low voltage did not enable the Taylor cone to rupture efficiently, this leads to larger fibers for smaller distances between plate and needle.

To analyze the effect of voltage on fiber diameter, we examine conditions 1, 2, 3 or 4, 5, 6 or 7, 8, 9 where each represents a series of fibers formed at voltages of 25, 20 and 15 kV. Higher voltage led to smaller diameter for each condition. At low voltages, the electrostatic force was not enough to pull all the fibers to the collector plate as many fibers fell between the gap of the collector plate and the needle. The thicker fibers at the lowest voltage indicate that there was not enough electrostatic force to completely overcome and break the Taylor cone on the tip of the needle. At a flow rate of 2.29 cm^3/h and tip distance from the collection plate of 15 cm, the fibers were not continuous. A combination of small fibers and jets of very large diameter fibers (~30 μm) were obtained. Increasing the magnitude of the flow rate preserved the trend of larger diameter fibers with decreased voltage (conditions 4, 5, 6 versus 1, 2, 3). However, a sharp decrease in the frequency of droplet formation was observed and resulted in a more uniform fabric formation. A similar breadth with a flatter distribution over the mean ranges was observed in the fiber diameters and a general trend of decreased diameter for the same voltage (condition 4 versus 1, 5 versus 2 and 6 versus 3) can be ascribed.

Increasing the magnitude of the flow rate while keeping voltage and distance between needle and plate can be examined by reviewing conditions 4, 5, 6 versus 1, 2, 3. A flatter distribution over the mean ranges was observed in the fiber diameters and a general trend of decreased diameter for the same voltage with increased flow rate (condition 4 versus 1, 5 versus 2 and 6 versus 2) can be described. As the flow rate is increased the Taylor cone is much bigger and the bursting of the Taylor cone gave much finer fibers. Comparing conditions in the histogram (1, 2 with 4, 5) we observe the frequency of thinner fibers increase as the flow rate is increased. For all conditions fibers with the highest frequency were less than or equal in number at high flow rates compared to low flow rates.

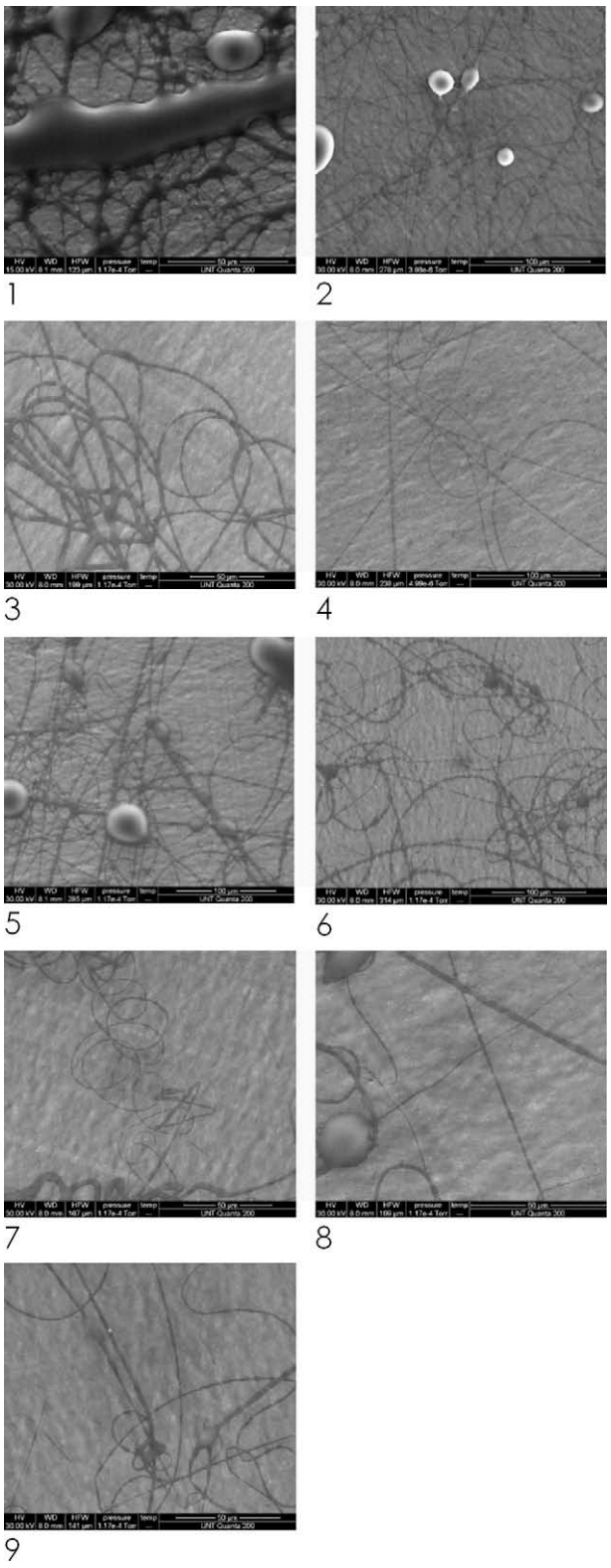

Fig. 3. SEM images of the electrospun fiber corresponding to Table 1.

4. XRD

XRD (Fig. 5) shows that levan powder is more crystalline than the fiber as indicated by the numerous peaks in the powder compared to the fiber. Fibers show a completely amorphous peak. We note that for electrospinning, a critical chain overlap concentration has been noted for polymers as a function of molecular weight (Gupta, Elkins, Long, & Wilkes, 2005). That is entanglements enable the charged polymer jet to retain its dimensional stability to the point of contact with the charged plate. For concentrations below this concentration, the charged polymer jet breaks into droplets or electrospraying is observed. This is similar to our experiments where concentrations less than 50% resulted in

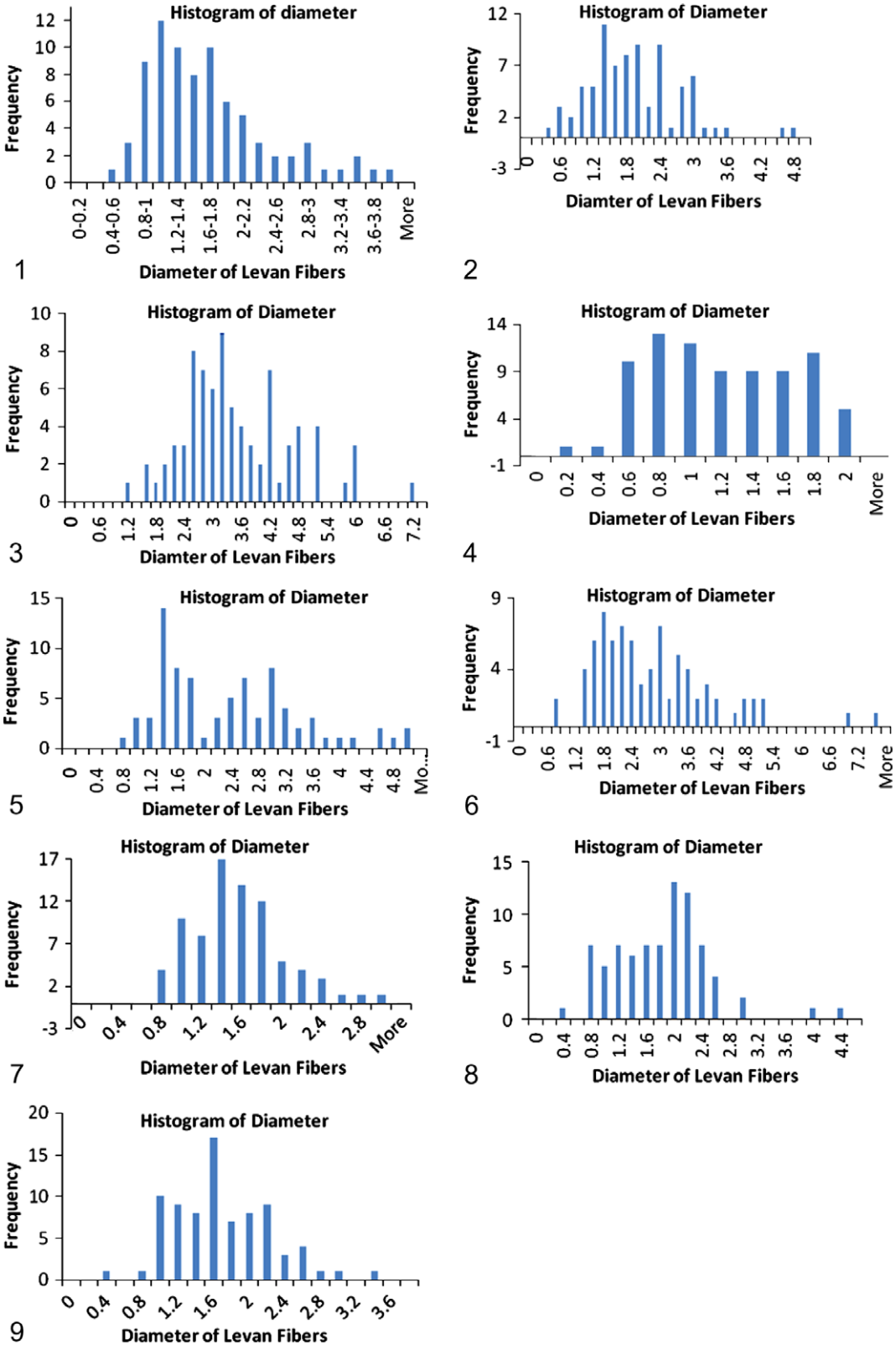

Fig. 4. Historgrams of the SEM images.

bead formation even at the highest voltage (20 kV). Only at high concentrations was fiber formation possible. We infer that the most likely reason for fiber formation is that chain entanglements occur at higher concentrations enabling the jet strength to be able to result in fiber formation.

5. Conclusion

Globules of the exopolysaccharide levan were dissolved in water. At a concentration of 60% by weight in deionized water, a transformation from crystalline to amorphous structure was en-

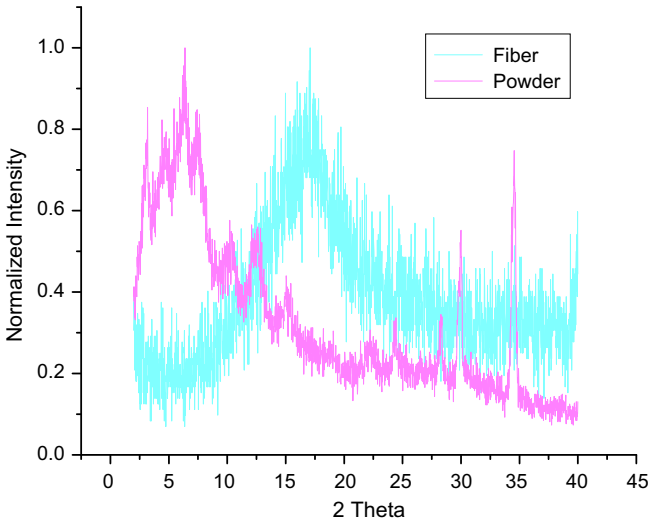

Fig. 5. XRD of Levan Powder and Fiber.

abled. Coupling the results of the rheology of levan (Arvidson et al., 2006) to the importance of chain entanglements for the transition from beads to fibers in electrospinning, we suggest that chain entanglements result in the fiber formation in levan. Increased voltage led to smaller fiber diameter. Increased flow rate and decreased distance between needle and charged plate, led to a larger fiber diameter.

Acknowledgements

Levan samples were provided by Montana Polysaccharides, Inc. of Winnsboro, SC. Financial support from DARPA is acknowledged. Center for Advanced Research and Technology (CART, UNT) instrumentation support is acknowledged.

Any opinions, findings and conclusions or recommendations expressed in this material are those of the authors and do not necessarily reflect the views of the Defence Advanced Research Projects Agency (DARPA); or its Contracting Agent, the US Department of the interior, National Business Center, Acquisition & Property Management Division, Southwest Branch. Distribution Statement "A" (Approved for Public Release, Distribution Unlimited).

References

Arvidson, S. A., Rinehart, B. T., & Gadala-Maria, F. (2006). Concentration regimes of solutions of levan polysaccharide from *Bacillus* sp.. *Carbohydrate Polymers, 144*, 149.

Combie, J. (2009). Personal communication.

Demir, M. M., Yilgor, I., & Erman, B. (2002). Electrospinning of polyurethane fibers. *Polymer, 43*, 3303–3309.

Desai, K., Kit, K., Li, J., & Zivanovic, S. (2008). Morphological and surface properties of electrospun chitosan nanofibers. *Biomacromolecules, 1000*, 1006.

Du, J., & Hsieh, Y.-L. (2008). Nanofibrous membranes from aqueous electrospinning of carboxymethyl chitosan. *Nanotechnology, 125707*, 125716.

Formhals, A. (1934). Patent No. 1,975,504. United States of America.

Frey, M. (2008). Electrospinning cellulose and cellulose derivatives. *Polymer Reviews, 378*, 391.

Gupta, P., Elkins, C., Long, T. E., & Wilkes, G. L. (2005). Electrospinning of linear homopolymers of poly (methyl methacrylate): Exploring relationships between fiber formation, viscosity, molecular weight and concentration in a good solvent. *Polymer, 46*, 4799–4810.

Jiang, H., Fang, D., Hsiao, B., Chu, B., & Chen, W. (2004). Optimization and characterization of dextran membranes prepared by electrospinning. *Biomacromolecules, 5*, 326–333.

Mo, X. M., Xu, C. Y., Kotaki, M., & Ramakrishna, S. (2004). Electrospun P(LLA-CL) nanofiber, a biomimetic extracellular matrix for smooth muscle cell and endothelial cell proliferation. *Biomaterials, 1883*, 1890.

Ploehn, H., personal communication.

Ritcharoen, W., Thaiying, Y., Saejeng, Y., Jangchud, I., Rangkupan, R., Meechaisue, C., et al. (2008). Electrospun dextran fibrous membranes. *Cellulose, 15*, 435–444.

Rutledge, G. C., Li, Y., Fridrikh, S., Warner, S. B., Kalayci, V. E., & Patra, P. (2001). *Electrostatic spinning and properties of ultrafine fibers*. National Textile Center Annual Report.

Song, J.-H., Kim, H.-E., & Kim, H.-W. (2008). Production of electrospun gelatin nanofiber by water-based co-solvent approach. *Journal of Materials Science. Materials in Medicine, 19*, 95–102.

Taylor, G. (1969). "Electrically driven jets". *Proceedings of the Royal Society of London, A. Mathematical and Physical Sciences, 313*, 453–475.

Woerdeman, D. L., Peng, Y., Shenoy, S., Parnas, R. S., Wnek, G. E., & Olga, T. (2005). Electrospun fibers from wheat protein: Investigation of the interplay between molecular structure and the fluid dynamics of the electrospinning process. *Biomacromolecules, 707*, 712.

Zhao, S. (2004). Electrospinning of ethyl cyano ethyl cellulose tetra hydro furan solution. *Journal of Applied Polymer Science, 242*, 246.